Published on 20 September 2016. Downloaded by University of Camerino on 29/09/2016 14:49:33.

CrystEngComm

PAPER

View Article Online
View Journal

Cite this: DOI: 10.1039/c6ce01598k

Rapid formation of single crystalline Ge nanowires by anodic metal assisted etching

S. J. Rezvani,*[abc] N. Pinto[ac] and L. Boarino[b]

Received 20th July 2016,
Accepted 20th September 2016

DOI: 10.1039/c6ce01598k

www.rsc.org/crystengcomm

Germanium nanowires are produced by a novel approach, combining two well known electrochemical and metal assisted chemical etching. The metal assisted etching procedure is enhanced by incorporation of HF in the catalytic solution and application of a constant bias to the substrate. Fast etching, caused by metal nanoparticles, facilitate pore nucleation for further pore growth. The improved current transport developed in the vicinity of the metal nanoparticles maintains a concentrated current density at the pore tip which results in an elongation of the pores in one direction and formation of long nanowires. With this new approach it is possible to fabricate nanowires with diameter below 100 nm and tens of micrometers long.

Semiconductor nanowires and particularly Ge nanowires (NW), due to their enhanced mobility, can improve the electrical and optical properties of one dimensional electronics and photovoltaics devices,[1–5] while being compatible with CMOS technology. Several techniques are currently used to fabricate Ge NWs, such as molecular beam epitaxy or chemical vapor deposition.[6–8] However, apart from the high cost, homogeneous production of NWs by these methods on a large area of a substrate, is still an open issue.[9–11] For instance, metal catalyst such as gold introduces deep impurity levels in semiconductor band gap altering the electronic transport properties of the wires.[12]

Metal assisted chemical etching (MAcE) is a simple and economically favored method currently used to fabricate Si NWs, offering a large variety of controllability over the Si wires parameters.[13,14] However, MAcE is not effective for Ge NWs fabrication. Although exact phenomena preventing Ge NWs by MAcE are not profoundly comprehended, it can be postulated to be attributed to the following factors. First, higher oxidation state of Ge (Ge^{4+}) compared with Si (Si^{2+}) which necessitates larger number of redox agents in the etching process. Second, water solubility of the germanium oxide that cease the mass transfer process by the disruption of the self-generated field at metal semiconductor interface. Third, the large leakage current which results in an isotropic etching of the Ge surface preventing the wire formation.[13,15] Recently, Föll *et al.* have proposed a method to fabricate long germanium nanowires by conventional electrochemical etching of the Ge substrate.[16] In the proposed method the nucleation of the germanium pore tip is a necessary step to commence the etching process. This necessitates a potential ramp in a very small range in which the pore is formed with a steady state condition for wire formation.[16] Moreover, the potential applied in the process should be managed to minimize transversal leakage current effects and keep the pore wall formation going. These obstacles make this method rather difficult to be realized in practice.

In the present work, a novel and simple approach for long Ge nanowire fabrication is introduced. The described procedure is a combination of the conventional metal assisted etching (MAcE) and electrochemical etching of the Ge substrate. Using this method, we have achieved Ge wires with diameters ranging from 10 to 300 nm and with a length up to 10 micrometers.

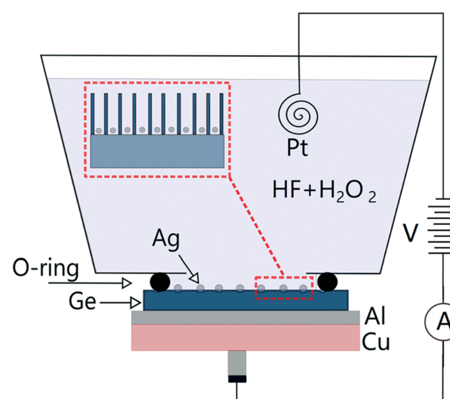

Fig. 1 Two electrodes standard etching cell experimental set-up consisting of an Al film as the back contact, sputtered on the back of the Ge wafer and annealed at 400 °C for 3–4 minutes to form an ohmic contact and a Pt electrode placed in the electrolytic solution. The setup was kept in dark and at a constant T = 25 °C.

[a] Scuola di Scienze e Tecnologie, Università di Camerino, 62032 Camerino, Italy. E-mail: seyedjavad.rezvani@unicam.it
[b] Istituto Nazionale di Ricerca Metrologica (INRiM), 10135 Torino, Italy
[c] Istituto Nazionale di Fisica Nucleare (INFN), Sezione di Perugia, Perugia, Italy

Published on 20 September 2016. Downloaded by University of Camerino on 29/09/2016 14:49:33.

All experiments were performed in a two electrode configuration electrochemical cell (see Fig. 1) using p-type doped Ge(100) wafers. Wafers were initially cleaned ultrasonically in acetone and methyl alcohol. Then they were exposed to a 10% HF solution in order to remove the native oxide layer. They were dipped in $AgNO_3$ solution for 10 seconds for Ag nanoparticles deposition afterwards (metal activation). All the experiments were carried out in a clean room with a constant temperature of 25 °C and in dark. The samples were analyzed by high resolution scanning electron microscopy (SEM) in plane and cross-section view.

In order to get an optimized pore density as a necessary prerequisite for wire formation, we carried out a specific two stage experiment. First the metal activated samples were etched using the standard MAcE solutions without an applied bias for pore formation optimization (see Table 1). Then starting from these optimized parameters, another set of fresh samples underwent a similar etching process but in presence of a constant applied bias. The results associated to each step are described and discussed in a separate section for a clearer interpretation of the mechanism involved in each step.

Pore nucleation

Pores formed by initial conventional MAcE of Ge substrates in a $HF:H_2O_2:H_2O$ (2 : 3 : 1) electrolyte without the applied bias are shown in Fig. 2a–c. The pores have a narrow size distribution and a surface density $\sim 1 \times 10^{16}$ cm^{-2} (Fig. 2f). The pores are square in shape with expected crystallographic side orientations along [110] and [1$\bar{1}$0] (Fig. 2d). They are also convex in shape due to the etching time gradient between top and bottom sidewalls and with {111} micro-facets to the side, positioned at an angle 54.7° (Fig. 2e).[15,17]

It is known that Ge wafers can be etched by conventional MAcE in H_2O_2 solution.[18] In an aqueous solution of Ag^+ salt (*e.g.*, $AgNO_3$, Ag_2SO_4, $AgClO_4$), Ag^+ is reduced to Ag particles on the Ge substrate and the Ge under Ag particles is catalytically etched into pores (Fig. 2). The Ge–Ge bonds act as the reducing agents for Ag^+ ions, resulting in the reduction of Ag^+ and the oxidation of Ge into Ge^{4+}.[13,19,20] The pore formation is originated in an enhanced electron transfer from Ge to O_2 around metallic particles and formation of water following the redox reactions:

$$2GeO + 4H^+ + 4e^- \leftrightarrow 2Ge + 2H_2O \quad (1)$$

Since GeO_2 is soluble in water the etching can be carried out without an acidic agent (HF). This etching usually results in pores with crystallographic micro-facets based on the crystalline orientation of the initial substrate.

On the other hand, in electrochemical etching of Ge, in presence of an applied bias and absence of metal particles, the anodic dissolution of Ge occurs in the form of tetravalent complex ions (*i.e.* the number of valence electrons of the overall reaction $n = 4$). Therefore, four holes are required to remove a Ge atom from the bulk p-type substrate with the following overall reaction:[21–23]

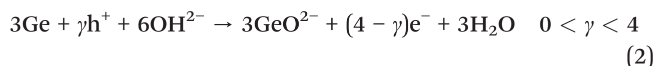

$$3Ge + \gamma h^+ + 6OH^{2-} \rightarrow 3GeO^{2-} + (4 - \gamma)e^- + 3H_2O \quad 0 < \gamma < 4 \quad (2)$$

It is shown that using HF can enhance the electrochemical etching process due to further dissolution of Ge oxide in HF.[24] In this model the tetravalent and divalent dissolution of Ge and Ge oxide in water and HF is accounted for as:

$$GeO_2 + H_2O \rightarrow H_2GeO_3 \quad \text{water-dissolution} \quad (3)$$

$$GeO + HF + 2e^- \rightarrow GeF^{2-} + xH + yOH \quad \text{HF-dissolution} \quad (4)$$

while reactions are significantly sensitive to the overall current density. In contrast to Si, the tetravalent dissolution is the main dissolution mechanism for current densities below 7.5 mA cm^{-2}.[25,26] With increasing etching current density, the divalent starts to dominate and at high current densities, the divalent dissolution becomes the main mechanism. In case of low etching current densities and long etching time, the solubility is only limited by HF concentration in which high concentrated electrolytes are able to dissolve large amount of Ge oxides. Considering the anodic dissolution enhancement at low current densities by HF contribution, it can be reasonably assumed that incorporation of HF in the electrolyte can also enhance the metal assisted etching process of Ge.

In our experiment we did many trials with different concentration of the redox agents and carefully analyzed the experimental data. We observed that MAcE etching in a conventional MAcE electrolyte solution ($HF:H_2O_2:H_2O$, 2 : 3 : 1) using Ag nanoparticles achieved from dipping Ge substrate in a 10 ml @ 10^{-4} ML $AgNO_3$ solution, results in a pore formation with a higher surface density and in a short time

Table 1 Summary of the resulted samples from 1) metal assisted chemical etching (MAcE); 2) anodic metal assisted chemical etching (AMAcE) and 3) electrochemical etching (EC) with different parameters used in our experiments

Etching method	Etching time	Catalytic solution	Metal particle-applied bias	Result
MAcE	1–5 min	$HF/H_2O_2/H_2O$	Ag – 0 V	Small crysto pores
MAcE	30 min	$HF/H_2O_2/H_2O$	Ag – 0 V	Large crysto pores
AMAcE	30 min	$HF/H_2O_2/H_2O$	Ag – 1.5 V	Long wires
AMAcE	30 min	HCl/H_2O	Ag – 1.5 V	Short wires
EC etching	30 min	$HF/H_2O_2/H_2O$	No metal – 1.5 V	Layer removal

This journal is © The Royal Society of Chemistry 2016

Published on 20 September 2016. Downloaded by University of Camerino on 29/09/2016 14:49:33.

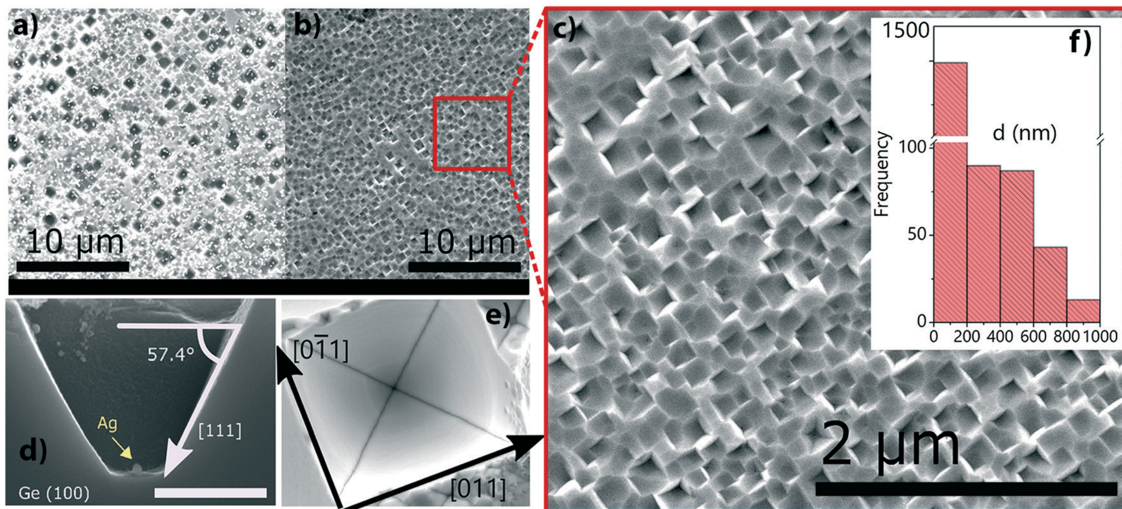

Fig. 2 a) SEM images of pore formation in Ge(100) sample etched by conventional MAcE for 5 minutes using Ag nanoparticles (small white dots) without an applied bias. b and c) Pores after removal of Ag nanoparticles. d) Cross section of crystallographic pores formed *via* MAcE showing the convex structure with {111} microfacets positioned at 57.4°. The scale bar is 300 nm. e) Top view showing the square shape of a pore formed with sides along [110] and [1$\bar{1}$0] directions. Scale bar is similar to panel (d). f) Size distribution of pores in panel (c) with a concentration at pore size ≤200 nm. Due to high number of pores below 200 nm, an axis break is inserted in the graph to show whole size distribution.

range (1–5 minutes) compared with H_2O_2. HF also enhances Ge dissolution and etching rate without altering the Ge atoms removal and selectivity with respect to the crystalline directions. Hence, the crystallographic pores (crysto pores) are expected to form as was observed in our samples. This high density Crysto pore formation by conventional MAcE can be used as the starting point (pore nucleation substitution) of Ge wire formation.

Wire formation

Wires fabricated by fresh metal activated samples in presence of the applied bias (AMAcE process) in $HF:H_2O_2:H_2O$; 2 : 3 : 1 solution are shown in Fig. 3a–e. A constant bias V_a = 1.5 V without ramping was used in our experiments. These samples show formation of nanowires by 30 minute etching. Nanowires have lengths up to 10 micrometers and they are

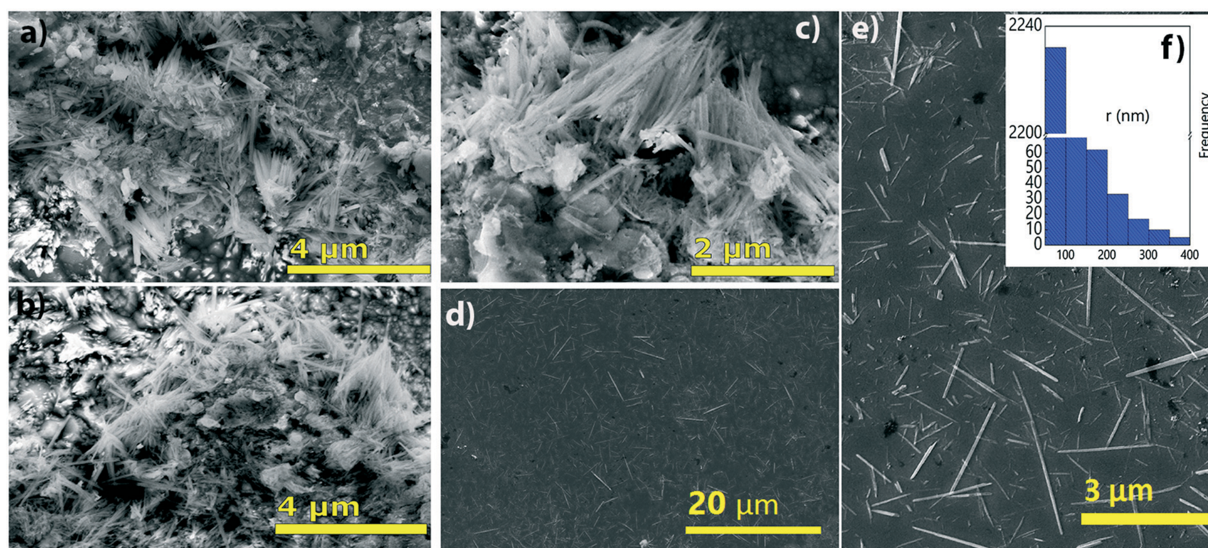

Fig. 3 SEM image of the wires formed by AMAcE etched for 30 minutes in ($HF:H_2O_2:H_2O$, 2 : 3 : 1) with a constant applied bias V_a = 1.5 V and titled at a) θ = 0°; b) θ = 10° and c) θ = 30°. d and e) In order to make a statistical analysis of the wire dimensions, they have been detached from the substrate and dispersed on a flat substrate. f) Diameter size distribution of the nanowires formed by AMAcE in HF/H_2O_2 with an average diameter ≤150 nm measured from panel (e). Due to a high frequency of the wires below 100 nm, an axis break is inserted in the graph to show the whole distribution range.

Published on 20 September 2016. Downloaded by University of Camerino on 29/09/2016 14:49:33.

oriented in the (100) direction depicting a current driven pore formation process. The diameter distribution of the wires are similar to that of the conventional MAcE pores prior to wires formation but with a smaller maximum. The majority of the wires have diameters below 100 nm (Fig. 3f).

The overall procedure of Ge nanowire formation by AMAcE approach can be summarized in three main steps (see Fig. 4) which will be discussed in details. First, the crystallographic pore formation in the absence of the applied bias within the first few seconds. Second, generation of the current transport at the pore tip by application of the external bias. Third, stabilized etching of the Ge substrate and formation of the nanowires along the current line.

Formation of nanowires by application of a constant bias to the metal activated samples cannot be simply explained in conventional electrochemical etching framework. In conventional Ge electrochemical etching, following the nucleation, for a subsequent pore growth, a constant potential and current cannot be easily optimized due to a large leakage current caused by Ge low band gap. The large leakage current dissolves the pore side walls and create a convex shape structure (similar to the conventional MAcE pores) preventing the formation of nanowires. Hence, to have a stable pore formation the current density should be kept constant and higher at pore tip compared with the transversal leakage current. This necessitates a constantly increasing current due to increase of the leakage current by the pore surface growth.

In case of AMAcE approach used in our experiment, formation of nanowires can be attributed to the role played by metal. The spontaneous nucleation of the pore tip by metal particles within few seconds (Step 1) facilitates the initiation of the etching process. The positive redox potential of the Ag enhances the hole injection to the Ge valence band[20] while the electrical field applied to the substrate will be highly localized by the metal curvature and the proton gradient across the metal surface as discussed in ref. 14, 27 and 28. The enhanced hole transport in the vicinity of the metal and a highly localized field at the pore tip can maintain a higher tip current density compared with the leakage current (Step II-see Fig. 4). These effects not only promote the formation of nanowires (Step III) but also leads to a faster etching rate (10 times faster) compared with the non-metal activated electrochemical etching of Ge, as long as the metal is in contact with the substrate. Our results also show that the applied bias below 0.5 V can not trigger the etching. This can be due to the fact that at quite low biases the tip current can not overcome the sidewalls leakage current that ceases the elongation of the pores.

The pore sidewalls are also expected to be etched with a lower rate that results in a radial growth of the pores and tapering of the wires. However, the large surface density of the pores developed by metal nanoparticles can easily drive the distance between two sidewalls to a value lower than twice of the space charge region (d_{SCR})

$$d_{SCR} = \sqrt{2\varepsilon\varepsilon_0 V_a / eN} \tag{5}$$

in which case the sidewalls become insulator and their etching ceases that results in stabilized formation of long nanowires.[15,29] In eqn (5), $\varepsilon\varepsilon_0$ is the dielectric constant of the Ge, V_a is the voltage drop across the space charge region, e is the electron charge and N is the dopant concentration of the Ge substrate.

To confirm the etching functionality by combination of two mechanisms we carried out further experiments that are summarized in Table 1. A metal activated sample was kept in HF/H_2O_2 solution for 30 minutes without any applied bias. Due to the lack of amplified pore current density by an accompanied bias the etching occurs in both direction and result in formation of large crysto pores up to 10 micrometers as shown in Fig. 5c and d. The sample shows formation of a very dense Ge micro-porous layer without any wires. Furthermore, a not metal activated Ge substrate was kept in a similar electrolyte for 30 minutes at V_a = 1.5 V and the sample showed simply removal of Ge layers from the surface. Finally, the results from HF/H_2O_2 electrolyte was also compared with high concentration (10%) HCl as the catalytic solution without the oxidant agent H_2O_2. The sample was etched for the same amount of time (30 min) and the same applied bias (1.5 V). It is known that in electrochemical etching of Ge with high concentration of the HCl, the –OH passivation is replaced by –Cl passivation, promoting (111) pore growth that are not suitable for the wire growth.[30,31] However, this sample also shows formation of nanowires but with a lower wire

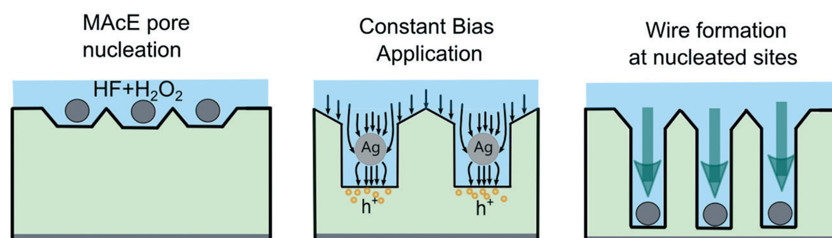

Fig. 4 Ge wire formation process by AMAcE method. Step I) High density of crystallographic pores are formed underneath the metal particles by conventional MAcE mechanism without an applied bias. Step II) Holes accumulate in vicinity of metal particles and a high current density will be built up at the Ge-metal interface (pore tip) due to the applied bias. Step III) Further Ge etching, driven by a stabilized current density, resulting in formation of Ge nanowires.

 This journal is © The Royal Society of Chemistry 2016

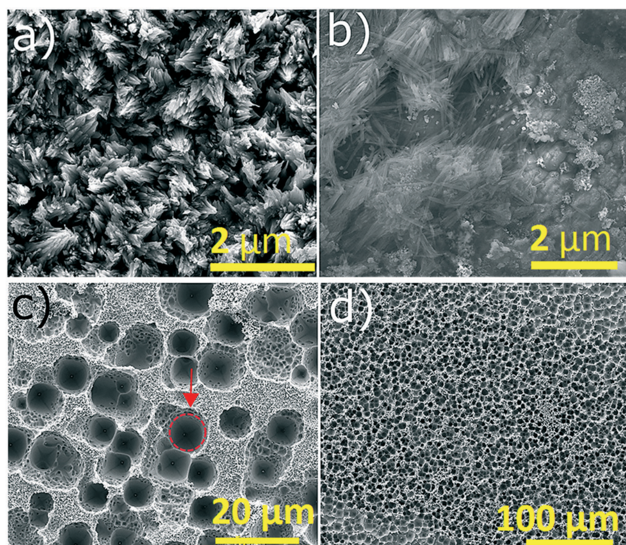

Fig. 5 a) Regions with crystallographic pores formed by AMAcE in HF/H_2O_2. b) SEM image of nanowires formed by AMAcE in 10% HCl solution after 30 minutes with a constant applied bias V_a = 1.5 V. c and d) Micropores formed by MAcE in 30 minutes by HF/H_2O_2 in absence of the applied bias. The pore shown by a circle in panel (c) can reach 10 microns in diameter; the large area view of the resulting pores are shown in panel (d).

density and shorter length compared with samples etched in HF electrolyte (see Fig. 5b). This can be the result of two effects. First, the –Cl passivation competing with the –OH passivation and effectively reducing the etching rate. Second, lower redox potential of HCl compared with HF/H_2O_2 results in formation of lower surface density of pores and hence lower density of wires. Moreover, the lower redox potential generates lower current density (holes) at the pore tip that further reduces the etching rate.

As a final remark, in samples with HF we also detected regions with crysto pores (see Fig. 5a). These small regions can be formed due to the following effects. First, the inhomogeneous distribution of the Ag nanoparticles both spatially and dimensionally. The Ag nanoparticles can agglomerate forming larger particles and regions with lower surface densities that create large pores to start with. These large pores can further be etched in a crystallographic manner due to lack of intense localized field at the low curvature of the large particles. Second, the nanoparticles (usually large particles) can be detached from the substrate surface after formation of the pore tip and also during the etching. This can result in continuation of the etching in a crystallographic direction with the lowest surface energy (usually [111]).

In summary, we have demonstrated the possibility of Ge nanowire fabrication by a novel method (AMAcE) combining conventional MAcE and electrochemical etching of crystalline Ge substrates. AMAcE is a simple, reliable and with high throughput of Ge NWs fabrication that can easily be integrated in the conventional nanotechnology. Ge NWs fabrication occurs within a two steps process. The first consisting in nucleation of pores with a well defined distribution of size and density by the conventional MAcE process. Wire formation sets in the second step only, *via* application of a suitable electrical potential to overcome the leakage current. Our results also depict the role of the localized field in proximity of the metal particles on the etching process that further improve the understanding of the MAcE and Electrochemical etching of Ge substrates.

Acknowledgements

Part of this research activity has been developed in the framework of the project 14IND01 3DMetChemIt, that has received funding from the EMPIR programme, co-financed by the Participating States and from the European Union's Horizon 2020 research and innovation programme. SEM micrographs have been produced by Nanofacility Piemonte INRiM, a laboratory supported by the Compagnia di San Paolo Foundation. This work is also partially funded by Camerino University project FAR 2012 CESEMN.

References

1 M. Yu, Y.-Z. Long, B. Sun and Z. Fan, Recent advances in solar cells based on one-dimensional nanostructure arrays, *Nanoscale*, 2012, **4**, 2783.
2 J. H. Lee, S. H. Choi, S. P. Patole, Y. Jang, K. Heo, W. J. Joo, J. B. Yoo, S. W. Hwang and D. Whang, Reliability enhancement of germanium nanowires using graphene as a protective layer: Aspect of thermal stability, *ACS Appl. Mater. Interfaces*, 2014, **6**, 5069–5074.
3 S. J. Rezvani, N. Pinto, E. Enrico, L. D'Ortenzi, A. Chiodoni and L. Boarino, Thermally activated tunneling in porous silicon nanowires with embedded Si quantum dots, *J. Phys. D: Appl. Phys.*, 2016, **49**, 105104.
4 J. Li, Y. Yu, C. Yue, S. Sun, W. Lin, H. Su, B. Xu, J. Li, S. Wu and J. Kang, The effects of different core-shell structures on the electrochemical performances of Si-Ge nanorod arrays as anodes for micro-lithium ion batteries, *ACS Appl. Mater. Interfaces*, 2014, **6**, 5884–5890.
5 J. Tang and K. L. Wang, Electrical spin injection and transport in semiconductor nanowires: challenges, progress and perspectives, *Nanoscale*, 2015, **7**, 4325–4337.
6 R. S. Wagner and W. C. Ellis, Vapor-Liquid-Solid Mechanism of Single Crystal Growth, *Appl. Phys. Lett.*, 1964, **4**, 89.
7 T. I. Kamins, X. Li, R. S. Williams and X. Liu, Growth and structure of chemically vapor deposited Ge nanowires on Si substrates, *Nano Lett.*, 2004, **4**, 503–506.
8 A. Rath, J. K. Dash, R. R. Juluri, A. Ghosh, T. Grieb, M. Schowalter, F. F. Krause, K. Muller, A. Rosenauer and P. V. Satyam, A study of the initial stages of the growth of au-assisted epitaxial Ge nanowires on a clean Ge(100) surface, *CrystEngComm*, 2014, **16**, 2486–2490.
9 S. J. Rezvani, N. Pinto, L. Boarino, F. Celegato, L. Favre and I. Berbezier, Diffusion induced effects on geometry of Ge nanowires, *Nanoscale*, 2014, 7469–7473.

Published on 20 September 2016. Downloaded by University of Camerino on 29/09/2016 14:49:33.

10 S. J. Rezvani, L. Favre, F. Celegato, L. Boarino, I. Berbezier and N. Pinto, Supersaturation state effect in diffusion induced Ge nanowires growth at high temperatures, *J. Cryst. Growth*, 2016, **436**, 51–55.
11 C.-Y. Tsai, S.-Y. Yu, C.-L. Hsin, C.-W. Huang, C.-W. Wang and W.-W. Wu, Growth and properties of single-crystalline Ge nanowires and germanide/Ge nano-heterostructures, *CrystEngComm*, 2012, **14**, 53–58.
12 N. Pinto, S. J. Rezvani, L. Favre, I. Berbezier, M. Fretto and L. Boarino, *Appl. Phys. Lett.*, 2016, **109**, 123101.
13 C. Chartier, S. Bastide and C. LevyClement, *Electrochim. Acta*, 2008, **53**, 5509–5516.
14 S. J. Rezvani, R. Gunnella, D. Neilson, L. Boarino, L. Croin, G. Aprile, M. Fretto, P. Rizzi, D. Antonioli and N. Pinto, Effect of carrier tunneling on the structure of si nanowires fabricated by metal assisted etching, *Nanotechnology*, 2016, **27**, 345301.
15 H. Föll, *et al.*, Electrochemical pore etching in germanium, *J. Electroanal. Chem.*, 2006, **589**, 259–288.
16 C. Fang, H. Föll and J. Carstensen, Long germanium nanowires prepared by electrochemical etching, *Nano Lett.*, 2006, **6**, 1578–1580.
17 T. Kawase, A. Mura, K. Dei, K. Nishitani, K. Kawai, J. Uchikoshi, M. Morita and K. Arima, Metal-assisted chemical etching of Ge(100) surfaces in water toward nanoscale patterning, *Nanoscale Res. Lett.*, 2013, **8**, 151.
18 M. Aizawa, A. M. Cooper, M. Malac and J. M. Buriak, Silver nano-inukshuks on germanium, *Nano Lett.*, 2005, **5**, 815–819.
19 X. Li and P. W. Bohn, *Appl. Phys. Lett.*, 2000, **77**, 2572.
20 Z. Huang, N. Geyer, P. Werner, J. De Boor and U. Gösele, Metal-assisted chemical etching of silicon: A review, *Adv. Mater.*, 2011, **23**, 285–308.
21 C. G. B. Garrett and W. H. Brattain, Physical theory of semiconductor surfaces, *Phys. Rev.*, 1955, **99**, 376–387.
22 W. H. Brattain and C. G. B. Garrett, Experiments on the Interface between Germanium and an Electrolyte, *Bell Syst. Tech. J.*, 1955, **34**, 129–176.
23 A. Uhlir, Electrolytic Shaping of Germanium and Silicon, *Bell Syst. Tech. J.*, 1956, **35**, 333–347.
24 E. Garralaga Rojas, J. Hensen, J. Carstensen, H. Föll and R. Brendel, Porous germanium multilayers, *Phys. Status Solidi C*, 2011, **8**, 1731–1733.
25 V. Lehmann, *Transport*, 2002, vol. 3, p. 283.
26 J. Carstensen, R. Prange, G. Popkirov and H. Föll, A model for current oscillations in the Si-HF system based on a quantitative analysis of current transients, *Appl. Phys. A: Mater. Sci. Process.*, 1998, **67**, 459–467.
27 K. Peng, J. Hu, Y. Yan, Y. Wu, H. Fang, Y. Xu, S. Lee and J. Zhu, *Adv. Funct. Mater.*, 2006, **16**, 387–394.
28 K. Kolasinski, The mechanism of galvanic/metal-assisted etching of silicon, *Nanoscale Res. Lett.*, 2014, **9**, 432.
29 C. Fang, H. Föll, J. Carstensen and S. Langa, Electrochemical pore etching in Ge - An overview, *Phys. Status Solidi A*, 2003, **204**, 1292–1296.
30 T. Hanrath and B. A. Korgel, Chemical surface passivation of Ge nanowires, *J. Am. Chem. Soc.*, 2004, **126**, 15466–15472.
31 H. Adhikari, P. C. McIntyre, S. Sun, P. Pianetta and C. E. D. Chidsey, Photoemission studies of passivation of germanium nanowires, *Appl. Phys. Lett.*, 2005, **87**, 1–3.

Published on 20 September 2016. Downloaded by University of Camerino on 29/09/2016 14:49:33.

 This journal is © The Royal Society of Chemistry 2016